THE EUROPEAN
PHYSICAL JOURNAL A

$A = 4 - 7\ \Xi$ hypernuclei based on interactions from chiral effective field theory

Hoai Le[2,a], **Johann Haidenbauer**[2,b], **Ulf-G. Meißner**[1,2,3,c], **Andreas Nogga**[2,d]

[1] HISKP and BCTP, Universität Bonn, 53115 Bonn, Germany
[2] IAS-4, IKP-3 and JHCP, Forschungszentrum Jülich, 52428 Jülich, Germany
[3] Tbilisi State University, 0186 Tbilisi, Georgia

Abstract We investigate the existence of bound Ξ states in systems with $A = 4 - 7$ baryons using the Jacobi NCSM approach in combination with chiral NN and ΞN interactions. We find three shallow bound states for the NNNΞ system (with $(J^\pi, T) = (1^+, 0)$, $(0^+, 1)$ and $(1^+, 1)$) with quite similar binding energies. The $^5_\Xi$H$(\frac{1}{2}^+, \frac{1}{2})$ and $^7_\Xi$H$(\frac{1}{2}^+, \frac{3}{2})$ hypernuclei are also clearly bound with respect to the thresholds ^{4}He + Ξ and ^{6}He + Ξ, respectively. The binding of all these Ξ systems is predominantly due to the attraction of the chiral ΞN potential in the $^{33}S_1$ channel. A perturbative estimation suggests that the decay widths of all the observed states could be rather small.

1 Introduction

Recent progress in strangeness $S = -2$ nuclear physics [1], in particular the observation of nuclear bound states of $\Xi^- - ^{14}$N ($^{15}_\Xi$C) [2–4] and possibly $\Xi^- - ^{11}$B ($^{12}_\Xi$Be) [5], and evidence from femtoscopic measurements for an attractive $\Xi^- p$ interaction [6,7] have again triggered considerable interest in studying Ξ hypernuclei theoretically [8–13] despite large uncertainties in the underlying ΞN interaction. The latter is due to the absence of direct hyperon-hyperon (YY) and ΞN scattering data, and the overall extremely scarce empirical information on $S = -2$ systems. There are several $\Lambda\Lambda$ hypernuclei unambiguously determined in experiments, with the s-shell $^6_{\Lambda\Lambda}$He [14,15] being the lightest one. Given huge challenges in experimental identifications of Ξ states, the possible existence of s-shell Ξ hypernuclei

remains by and large an open question. Thus, theoretical predictions for Ξ hypernuclei especially for light systems are of great importance. Results from such studies can provide useful guidelines for experimentalists in searching for Ξ bound states.

In this work we explore the possible existence of light Ξ hypernuclei up to $A = 7$. For the lightest system, $^3_\Xi$H, several calculations can be found in the literature [16–19]. Not surprisingly, the predictions strongly depend on the interaction models used. For example, Garcilazo et al. [16] and Hiyama et al. [18] both obtained a deeply bound $^3_\Xi$H $(J^\pi = 3/2^+, T = 1/2)$ state employing an effective ΞN potential that mimics the phase shifts of the Nijmegen ESC08c potential [20]. On the other hand, for interactions derived within chiral effective field theory (EFT) [21] or for ΞN potentials deduced from lattice QCD simulations by the HAL QCD Collaboration [22], the system is found to be unbound [18,19]. It has to be said that a strongly attractive ΞN force as suggested by that ESC08c potential, which even yields a ΞN two-body bound state [20], is not supported by the currently available empirical constraints [23] including the aforementioned femtoscopic measurements, and also not by lattice simulations at almost physical masses [22]. Note that in the work by Miyagawa et al. [19] the original ΞN interactions have been used directly to obtain the t matrices entering the Faddeev equations for the three-baryon bound state. For the solution of these equations, however, only ΞNN channels are considered. The variational calculation of Hiyama et al. [18] is based on interactions where the various YY channels of the original potential models [20,22] are renormalized into an effective ΞN interaction and where the latter is then treated within the so-called Gaussian expansion method [24]. Earlier studies of Ξ hypernuclei with $A = 5 - 12$ by Hiyama et al. were performed within a cluster model [25].

[a] e-mail: h.le@fz-juelich.de (corresponding author)

[b] e-mail: j.haidenbauer@fz-juelich.de

[c] e-mail: meissner@hiskp.uni-bonn.de

[d] e-mail: a.nogga@fz-juelich.de

In the present study, we will employ the Jacobi no-core shell model (J-NCSM) in combination with microscopic nucleon–nucleon (NN) and YY-ΞN interactions derived within chiral EFT to investigate $A = 4 - 7$ Ξ hypernuclei. Chiral EFT [26] is a very powerful tool for precisely describing the NN interaction (see [27] and references therein) and allows for accurate calculations of nuclear observables [28–31]. It has also been successfully utilized in studies of the ΛN and ΣN interactions by the Jülich–Bonn–Munich group [32–34]. These chiral YN potentials have already been used to study Λ hypernuclei within the J-NCSM approach up to the p-shell [35,36]. Likewise, the YY-ΞN potentials from chiral EFT up to NLO [21,23] yield promising results for s-shell $\Lambda\Lambda$ hypernuclei [37]. Therefore, it is very interesting to explore the predictions of chiral EFT for Ξ hypernuclei, in particular for light systems where a microscopic (ab initio) treatment is possible.

The paper is organized as follows: in the next section we describe the baryon–baryon (BB) interactions employed in this work focusing particularly on the $S = -2$ BB potentials. Section 3 contains a brief description of the J-NCSM and its application to Ξ hypernuclei, and of the method to extrapolate the binding and separation energies to infinite model spaces. In Sect. 4, our results for NNNΞ, $^5_\Xi$H and $^7_\Xi$H are discussed. Final conclusions are given in Sect. 5. In Appendix A, we provide approximately valid expressions for the partial-wave contributions if the ΞN interactions to s-shell Ξ hypernuclei.

2 Baryon–baryon interactions for $S = -2$

For all calculations presented here, we employ BB interactions that are derived within chiral EFT [26]. The high-order semilocal momentum-space regularized potential with a regulator of $\Lambda_N = 450$ MeV (N^{4}LO+(450)) [27] is used for the NN interaction. For the interaction in the ΞN channel, we employ the potential from Ref. [21]. This interaction for the $S = -2$ sector has been constructed in agreement with empirical constraints on the $\Lambda\Lambda$ S-wave scattering length and with published values and upper bounds for $\Xi^- p$ elastic and inelastic cross sections [23]. Moreover, it yields a moderately attractive Ξ-nuclear interaction as suggested by experimental evidence for the existence of Ξ-hypernuclei [2,4]. The value obtained for the Ξ single-particle potential $U_\Xi(k = 0)$ at nuclear matter saturation density is with around -9 MeV [38] noticeably smaller than the commonly cited potential depth of -14 MeV [39,40]. An application of this single-particle potential to finite Ξ nuclei based on the local density approximation method [12,38] showed, however, that pertinent predictions for the aforementioned recently reported states [2–4] are quite in line with the energies observed in the experiments.

The considered ΞN interaction includes the coupling to other BB channels in the strangeness $S = -2$ sector ($\Lambda\Lambda$, $\Lambda\Sigma$, $\Sigma\Sigma$). However, in the actual calculation within the J-NCSM, it turned out that convergence of the eigenvalue iterations (that diagonalize the many-body Hamiltonian) to the lowest lying Ξ states is rather poor when the coupling of ΞN to $\Lambda\Lambda$ is explicitly included. Thus, similar to what has been done by Hiyama et al. [18,25], the explicit coupling to $\Lambda\Lambda$ is omitted. Instead, the contribution from the transition $\Lambda\Lambda - \Xi$N, which anyway can occur only in the $^1S_0$ partial wave with isospin $I = 0$, is incorporated effectively by re-adjusting the strength of the corresponding $V_{\Xi N - \Xi N}$ potential. The other channel couplings in the $S = -2$ sector, i.e. ΞN $- \Lambda\Sigma - \Sigma\Sigma$, are, however, still taken into account. In practice, the S-wave low-energy constants (LECs) in the $I = 0$ channel (to be concrete, those corresponding to the SU(3) singlet irrep. {1} [23,41]) are appropriately re-adjusted so that the real part of the ΞN scattering length remains practically the same after omitting the $\Lambda\Lambda$ channel.

Nonetheless, there is a delicate issue connected with that step. The chiral EFT interaction at NLO predicts the existence of a virtual state in the $I = 0$, $^1S_0$ wave extremely close to the ΞN threshold [21,23]—a possible remnant of the H-dibaryon [42]. The virtual state is reflected in an impressive cusp structure in the $\Lambda\Lambda$ phase shift and a large ΞN phase [23]. The pertinent ΞN scattering length is large too, cf. Table 1 in Ref. [21], with an imaginary part in the order of 10 fm or more. Similar features are also seen in lattice QCD results [22]. The large imaginary part somehow suggests an overall strong $\Lambda\Lambda - \Xi$N coupling. However, its value is artificially enhanced by the near-by virtual state. This can be easily seen by performing the calculation in the particle basis and with physical masses. Then the cusp is strongly reduced [23], and the scattering lengths in the Ξ^0n channel amount to $a = (-1.30 - i\,0.07)$ fm, $(-2.05 - i\,0.27)$ fm, $(-1.95 - i\,0.25)$ fm, $(-1.41 - i\,0.09)$ fm, respectively, for the cutoffs $\Lambda = 500$, 550, 600, and 650 MeV in the regulator function considered in [21,23]. Obviously, now the imaginary part is rather small and that means the actual $\Lambda\Lambda - \Xi$N coupling is indeed fairly weak. The latter conclusion has also been drawn in Ref. [19] where this issue has been examined from a slightly different perspective. See also the discussion in Ref. [12].

For the present exploratory study, we chose the YY-ΞN NLO potential with the cutoff of $\Lambda = 500$ MeV, i.e. the interaction with the smallest imaginary part. Moreover, we adjusted the LECs to the Ξ^0n scattering length, instead of the one for $I = 0$, in order to avoid any strong bias from the actual but unsettled location of the virtual state. After the re-adjustment the $^{11}S_0$ potential, using the notation $^{(2I+1)(2S+1)}L_J$, yields $a_{\Xi N}(^{11}S_0) = -7.00$ fm, to be compared with $a_{\Xi N}(^{11}S_0) = -7.71 - i\,2.03$ fm for the original potential where all coupled channels are considered [21]. We

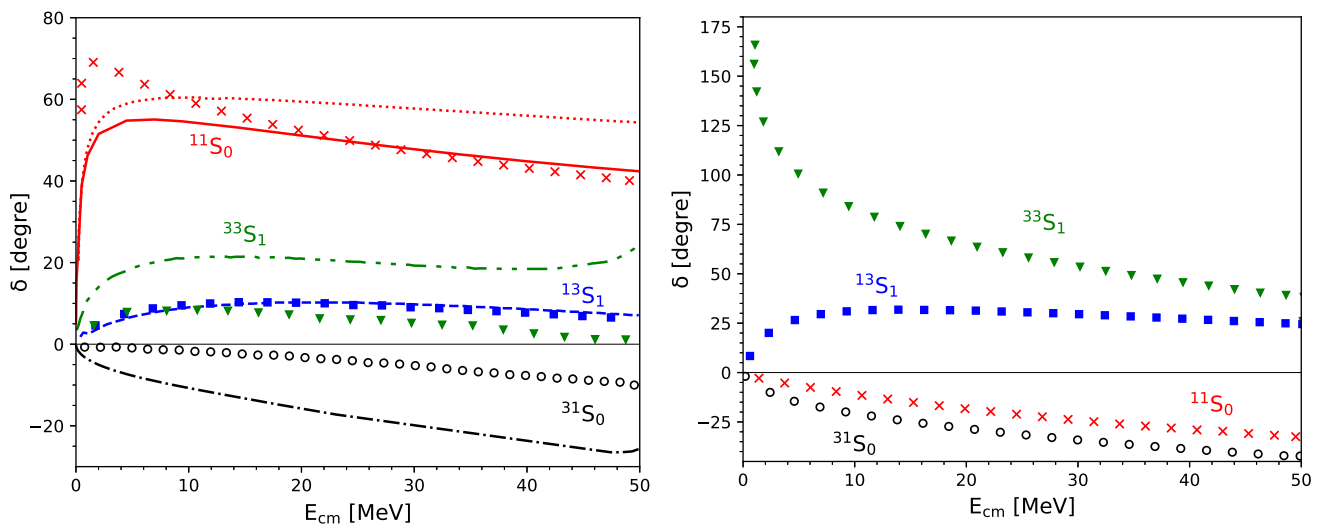**Fig. 1** ΞN phase shifts predicted by the NLO(500) and HAL QCD potentials (left panel) compared to those of the Nijmegen ESC08c model (right panel). The NLO(500) results are shown by lines: $^{11}S_0$ (dotted, red), $^{31}S_0$ (dash-dotted, black), $^{13}S_1$ (dashed, blue) and $^{33}S_1$ (dash-double-dotted, green). The solid line indicates the $^{11}S_0$ phase shift of the re-adjusted NLO(500) potential, see text. The HAL QCD and ESC08c results (values are taken from [18]) for $^{11}S_0$, $^{31}S_0$, $^{13}S_0$ and $^{33}S_0$ are indicated by crosses, circles, squares, and triangles, respectively. Note the different scales in the left and right panels

believe that this procedure allows us to capture the essential features of the chiral ΞN interaction in the $^{11}S_0$ channel reliably, while guaranteeing at the same time the applicability of the J-NCSM approach. Note that all other ΞN partial waves are not affected by this modification anyway and $\Lambda\Sigma$ and $\Sigma\Sigma$ components are included in the J-NCSM calculations. We, however, neglect YN interactions that are expected to give insignificant contributions but could potentially again induce $\Lambda\Lambda$ components to the many-body state. We postpone a more thorough investigation on this issue and of the dependence of the Ξ binding energies on the chiral cutoff Λ_{YY} to a future study.

Finally, to speed up the convergence of the J-NCSM calculations, the NN and YY interactions are evolved using the similarity renormalization group (SRG) [43]. Thereby, we use an SRG flow parameter of $\lambda_{NN} = 1.6$ fm^{-1} for the NN interaction. This value has already been used in Refs. [36,37] and is motivated by the observation that ordinary nuclei are bound fairly realistically even if three-nucleon forces are neglected for this λ_{NN}. The $S = -2$ potential is SRG-evolved to a wide range of SRG flow parameter (denoted generically by λ_{YY}), namely $1.4 \leq \lambda_{YY} \leq 3.0$ fm^{-1}. The variations of the binding energies with respect to λ_{YY} allow one to quantify the possible contribution of the omitted SRG-induced three- and more-body forces. Note that such contributions are remarkably small for $\Lambda\Lambda$ hypernuclei [37]. We also explicitly take into account the electromagnetic NN interaction [44] as well as the Coulomb point-like interaction between Ξ^- and proton. These interactions are however not included in the SRG evolution but only added afterwards.

It is worthwhile to compare the ΞN phase shifts of the employed EFT interaction NLO(500) with those predicted by the Nijmegen ESC08c [20] and the HAL QCD [22] potentials. As mentioned in the introduction, the latter two interactions have recently been considered in $A = 3, 4$ Ξ hypernuclear calculations by Hiyama et al. [18]. The phase shifts for the four S-wave states, namely $^{11}S_0$, $^{31}S_0$, $^{13}S_1$ and $^{33}S_1$, are displayed in Fig. 1. As expected, the original NLO(500) interaction (cf. the dotted line) and the re-adjusted potential differ only slightly in the $^{11}S_0$ phase shifts. Overall, the results by the NLO(500) and HAL QCD interactions are qualitatively similar to each other, but differ substantially from those of the Nijmegen ESC08c potential. The ESC08c is strongly attractive in the $^{33}S_1$ channel (leading to a deuteron-like ΞN bound state), whereas the chiral NLO(500) (HAL QCD) interaction is only moderately (weakly) attractive in this channel. Moreover, while the $^{11}S_0$ ΞN interaction is rather attractive in the HAL QCD and NLO(500) potentials, it is actually repulsive in the ESC08c model. Although the NLO(500) and HAL QCD ΞN phase shifts exhibit an overall similar trend, there are visible differences in all ΞN partial waves except for $^{13}S_1$ where there are no channel couplings. As we will discuss later, such variations lead to qualitative differences in the predictions of the two interactions for light Ξ systems.

3 Jacobi NCSM for Ξ hypernuclei

The application of the J-NCSM to Ξ hypernuclei follows very closely our J-NCSM formalism for $\Lambda\Lambda$ systems described in [37]. Here we also split the basis functions into two orthogonal sets: one set that involves two $S = -1$ hyperons, $|\alpha^{*(Y_1 Y_2)}\rangle$, and the other that contains the doubly strange Ξ hyperon, $|\alpha^{*(\Xi)}\rangle$. The $|\alpha^{*(\Xi)}\rangle$ states are exactly the same as constructed in [37],

$$
\begin{aligned}
|\alpha^{*(\Xi)}\rangle &= |\alpha_{(A-1)N}\rangle \otimes |\Xi\rangle \\
&= |\mathcal{N} J T, \alpha_{(A-1)N} \, n_\Xi \, I_\Xi \, t_\Xi; \\
&\quad (J_{A-1}(l_\Xi \, s_\Xi) \, I_\Xi) J, (T_{A-1} \, t_\Xi) T\rangle .
\end{aligned} \tag{1}
$$

Since the $\Lambda\Lambda - \Xi N$ transition is absorbed into the strength of the $V_{\Xi N - \Xi N}$ potential and since we omit YN interactions, the basis states $|\alpha^{*(Y_1 Y_2)}\rangle$ can be restricted to

$$
\begin{aligned}
|\alpha^{*(Y_1 Y_2)}\rangle &= |\alpha_{(A-2)N}\rangle \otimes |Y_1 Y_2\rangle \\
&= |\mathcal{N} J T, \alpha_{(A-2)N} \, \alpha_{Y_1 Y_2} \, n_\lambda \lambda; \\
&\quad ((l_{Y_1 Y_2}(s_{Y_1} s_{Y_2}) S_{Y_1 Y_2}) J_{Y_1 Y_2}(\lambda J_{A-2}) I_\lambda) J, \\
&\quad ((t_{Y_1} t_{Y_2}) T_{Y_1 Y_2} T_{A-2}) T\rangle,
\end{aligned} \tag{2}
$$

with $|Y_1 Y_2\rangle = |\Lambda\Sigma\rangle$ or $|\Sigma\Sigma\rangle$. The notations used in Eqs. (1,2) are the same as in [37].[1] For example, the symbol $\alpha_{(A-2)N}$ stands for all quantum numbers characterizing the antisymmetrized states of $A - 2$ nucleons: the total number of oscillator quanta $\mathcal{N}_{A-2}$, total angular momentum J_{A-2}, isospin T_{A-2} and state index ζ_{A-2} as well. Similarly, $\alpha_{Y_1 Y_2}$ stands for a complete set of quantum numbers describing the subcluster of two hyperons Y_1 and Y_2. The principal quantum number n_λ of the harmonic oscillator (HO) together with the orbital angular λ describe the relative motion of the $(A-2)$N core with respect to the center-of-mass (C.M.) of the $Y_1 Y_2$ subcluster. The orders, in which these quantum numbers are coupled, are shown after the semicolon.

For practical calculations, we truncate the model space by limiting the total HO energy quantum number $\mathcal{N}$ in Eqs. (1,2) to $\mathcal{N} \leq \mathcal{N}_{max}$ where $\mathcal{N} = \mathcal{N}_{A-2} + 2n_\lambda + l_\lambda + \mathcal{N}_{Y_1 Y_2}$ or $\mathcal{N} = \mathcal{N}_{A-1} + l_\Xi + 2n_\Xi$, respectively. As a consequence, the computed binding energies will depend on $\mathcal{N}_{max}$ and on the HO frequency ω. To extract the converged results we will follow the two-step extrapolation procedure that has been successfully employed for nuclear and hypernuclear energy calculations [36,37,45]. First, the energies $E(\mathcal{N}, \omega)$ are computed for all accessible model spaces $\mathcal{N}_{max}$ and for a wide range of ω. Then $E_\mathcal{N}$ is determined for a given $\mathcal{N}_{max} = \mathcal{N}$ by minimizing the energies $E(\mathcal{N}, \omega)$ with respect to ω. In the second step, an exponential fit is applied to $E_\mathcal{N}$ in order to extrapolate to $\mathcal{N} \to \infty$.

---

[1] To be consistent with [37] we use here and later on t, T for the isospins.

Furthermore, in order to write down the explicit form of the Hamiltonian, we also distinguish three parts of the Hamiltonian, namely $H_{Y_1 Y_2}$, H_Ξ and $H_{Y_1 Y_2, \Xi N}^{S=-2}$, like for $\Lambda\Lambda$ hypernuclei. As mentioned before, we do not take into account YN interactions in the $S = -1$ sector here. Hence, the $H_{Y_1 Y_2}$, $H_{Y_1 Y_2, \Xi N}^{S=-2}$ and H_Ξ can be written as

$$
\begin{aligned}
H_{Y_1 Y_2} &= \sum_{i<j=1}^{A-2} \left(\frac{2p_{ij}^2}{M(t_{Y_1}, t_{Y_2})} + V_{ij}^{S=0} \right) \\
&\quad + \frac{m(t_{Y_1}) + m(t_{Y_2})}{M(t_{Y_1}, t_{Y_2})} \frac{p_{Y_1 Y_2}^2}{2\mu_{Y_1 Y_2}} + V_{Y_1 Y_2}^{S=-2} \\
&\quad + \left(m(t_{Y_1}) + m(t_{Y_2}) - m_\Xi - m_N \right),
\end{aligned} \tag{3}
$$

$$
H_{Y_1 Y_2, \Xi N}^{S=-2} = \sum_{i=1}^{A-1} V_{Y_1 Y_2, \Xi i}^{S=-2}, \tag{4}
$$

$$
\begin{aligned}
H_\Xi &= H_\Xi^{S=0} + H_\Xi^{S=-2} \\
&= \sum_{i<j=1}^{A-1} \left(\frac{2p_{ij}^2}{M(\Xi)} + V_{ij}^{S=0} \right) \\
&\quad + \sum_{i=1}^{A-1} \left(\frac{m_N + m_\Xi}{M(\Xi)} \frac{p_{\Xi i}^2}{2\mu_{\Xi i}} + V_{\Xi i}^{S=-2} \right),
\end{aligned} \tag{5}
$$

with $|Y_1 Y_2\rangle = |\Lambda\Sigma\rangle$ or $|\Sigma\Sigma\rangle$. Here, $m(t_{Y_1})$, $m(t_{Y_2})$, m_Ξ and m_N are the Y_1, Y_2, Ξ hyperon and nucleon rest masses, respectively. M denotes the total rest mass of the system, thus, $M(t_{Y_1}, t_{Y_2}) = m(t_{Y_1}) + m(t_{Y_2}) + (A - 2)m_N$ and $M(\Xi) = m_\Xi + (A-1)m_N$. $\mu_{i\Xi}$ and $\mu_{Y_1 Y_2}$ are the ΞN and YY reduced masses, respectively. The rest mass differences within the nucleon- and hyperon-isospin multiplets are neglected. $V^{S=0}$ and $V^{S=-2}$ are the two-body NN and YY (ΞN) potentials. Finally, the last term in Eq. (3) accounts for the difference in the rest masses of the hyperons arising due to particle conversions.

With the basis states defined in Eqs. (1,2), the matrix elements of the Hamiltonian Eqs. (3–5) can be evaluated analogously as done in [37]. Likewise, the final Ξ wave functions and the corresponding binding energies are directly obtained via the Lanczos eigenvalue iterations.

4 Results and discussion

As it has been shown in [19], the $^3_\Xi$H hypernucleus is not bound with the chiral YY-ΞN NLO potential [21]. Therefore, the lightest system that we study here is NNNΞ. A Ξ hyperon with isospin $\frac{1}{2}$ can couple to the core nucleus ^{3}H/^{3}He in its ground state $(\frac{1}{2}^+, \frac{1}{2})$ resulting in several NNNΞ states with $(J^\pi, T) = (1^+, 0)$, $(0^+, 1)$, $(1^+, 1)$ and $(0^+, 0)$. The first three states are found to be strongly bound in the work by Hiyama et al. when the Nijmegen ESC08c potential is used. The HAL QCD potential, however, supports only one weakly

bound $NNN\Xi$ state, namely the $(1^+, 0)$ [18]. As discussed in Sect. 2, there are some differences in the predictions for the ΞN phase shifts by the NLO(500) and HAL QCD interactions. It is therefore interesting to calculate the $A = 4$ system based on the chiral potential in order to see whether such differences are manifest in the predictions for the $NNN\Xi$ binding energies. We also consider $^{5}_{\Xi}$H. Due to the strong binding of the α particle core, the mass difference between ΞN and $\Lambda\Lambda$ is partly removed [46] which makes this light hypernucleus especially interesting. Likewise, theoretical predictions for $^{7}_{\Xi}$H are timely and of importance. The authors in [25] have proposed to produce $^{7}_{\Xi}$H using the (K^-, K^+) reaction on the ^{7}Li target. Also the upcoming experiment at J-PARC [47] is devoted to study the $^{5}_{\Lambda\Lambda}$H hypernucleus formed via the decay of $^{7}_{\Xi}$H using the same reaction. Generally, we expect that a consistent study of hypernuclei for a range of mass numbers might provide constraints for the properties of the Ξ hyperon in nuclear matter. In this work, we present such an investigation for Ξ hypernuclei up to $A = 7$.

In this exploratory study, we do not take the $\Xi^- - \Xi^0$ mass difference of 6.85 MeV into account and assume isospin symmetry by assigning to each state a definite isospin. We believe that this is justified to identify states that are possibly bound but stress that the impact of the mass difference and possible isospin breaking by other contributions like the Coulomb interaction should be analysed in a future study. For the $A = 3$ and $A = 5$ Ξ hypernuclei, the isospins are well defined since the corresponding core nucleus is predominantly in its isospin zero state. For $A = 7$, we follow the choice of Hiyama et al. [18] and only consider the $(1/2^+, 3/2)$ state. For this state, it is natural to expect that the $\Xi^- - {}^6$He$(0^+, 1)$ component is the dominant one. The situation is less clear for $A = 4$ since, a priori, none of the possible isospins is favored by the 3N core. Below we have therefore assumed isospin symmetry and give separate results for $T = 0$ and $T = 1$ states. Our results for the contribution of the Coulomb interaction suggest that this is a reasonable approximation since the binding is still predominately due to the strong interaction. However, a more careful analysis also taking the cascade mass difference into account should be performed in the future.

As mentioned earlier, in order to eliminate the effect of finite-basis truncation on the binding energies, we follow the two-step extrapolation procedure as explained in [36]. The ω- and $\mathcal{N}$-space extrapolations for the binding energy of the $^{4}_{\Xi}$H$(1^+, 0)$ state, $E(1^+, 0)$, are illustrated in panels (a) and (b) of Fig. 2, respectively. To obtain the converged Ξ separation energy B_{Ξ}, we perform an analogous exponential fit on the quantities $B_{\Xi}(\mathcal{N}) = E_{\mathcal{N}}(1^+, 0) - E_{\mathcal{N}}(^3\text{H})$, see also panel (c). Here $E_{\mathcal{N}}(1^+, 0)$, $E_{\mathcal{N}}(^3\text{H})$ are the hypernuclear and nuclear binding energies, respectively, obtained at their optimal HO frequencies for a given model space $\mathcal{N}$. For the separation energies, we cannot expect a monotonic convergence a priori. But for the results shown here, we observed that this is the case and that an exponential fit is appropriate. The same approach was used for the separation energies obtained in our earlier studies [36,37]. Note that the error bars shown in panels (b)–(c) are given by the difference to the next model space. These error bars are not meant to provide a realistic uncertainty estimate, but rather to assign relative weights for the following extrapolation to $\mathcal{N} \to \infty$. Clearly, well-converged results for both $E(1^+, 0)$ and $B_{\Xi}(1^+, 0)$ are achieved for model spaces up to $\mathcal{N}_{max} = 30$. For the NN interaction alone, the triton energy calculation is, however, converged already for model spaces $\mathcal{N}_{max} = 24$. Similar convergence patterns are also observed for the binding (separation) energies of the other states in $NNN\Xi$ and of the $^{5}_{\Xi}$H$(\frac{1}{2}^+, \frac{1}{2})$, $^{7}_{\Xi}$H$(\frac{1}{2}^+, \frac{3}{2})$ hypernuclei. The convergence for $A = 5$ and $A = 7$ is generally faster since the separation energies are larger. Therefore, our current limits of $\mathcal{N}_{max} = 16$ and 12 for $A = 5$ and 7, respectively, still allow an accurate determination of the energies as can be seen from Table 1.

In order to minimize the contribution of the Coulomb interaction, we use the $^{4}_{\Xi}$n states for isospin $T = 1$. As can be seen in Table 1, both of these states, $^{4}_{\Xi}$n$(0^+, 1)$ and $^{4}_{\Xi}$n$(1^+, 1)$, are clearly bound for the chiral interaction. It turns out that their binding energies are comparable to the one for $^{4}_{\Xi}$H$(1^+, 0)$. The $^{4}_{\Xi}$H$(0^+, 0)$ state, on the other hand, is unbound for the chiral interactions at NLO.

The converged $B_{\Xi}(1^+, 0)$ computed for a wide range of SRG-flow parameter, $1.4 \leq \lambda_{YY} \leq 3.0$ fm^{-1}, are presented in panel (d) of Fig. 2. One sees that the overall variation of $B_{\Xi}(1^+, 0)$ is visible, about 190 ± 30 keV. It is also larger than the dependence of $B_{\Lambda\Lambda}$ on the SRG-flow parameter, which was found to be of the order of 100 keV [36]. This may be related to the fact that, unlike for the $\Lambda\Lambda$ case where the coupling to the pion is suppressed by isospin conservation, π exchange contributes to the ΞN interaction at leading order. Long-range interactions are likely to be more strongly affected by the SRG evolution. However, the variation is much smaller than the one observed for single Λ hypernuclei (see e.g. [36]). For the $A = 5$ and 7 Ξ hypernuclei, we observed similarly large absolute variations, but still they are relatively smaller as compared to the estimated Ξ separation energies. Therefore, in all cases, the SRG dependence is small enough that it does not affect conclusions on the existence of the found bound states. Thus, in the following discussion, we will present results for a specific flow parameter, namely $\lambda_{YY} = 1.6 \, fm^{-1}$. Anyway, in the future, it will be interesting to better explore the dependence on the SRG evolution. Such calculations are however beyond the scope of the current work.

The predicted separation energies B_{Ξ} for the $A = 4 - 7$ Ξ hypernuclei are listed in Table 1. We verified that all the bound states established here are predominantly due
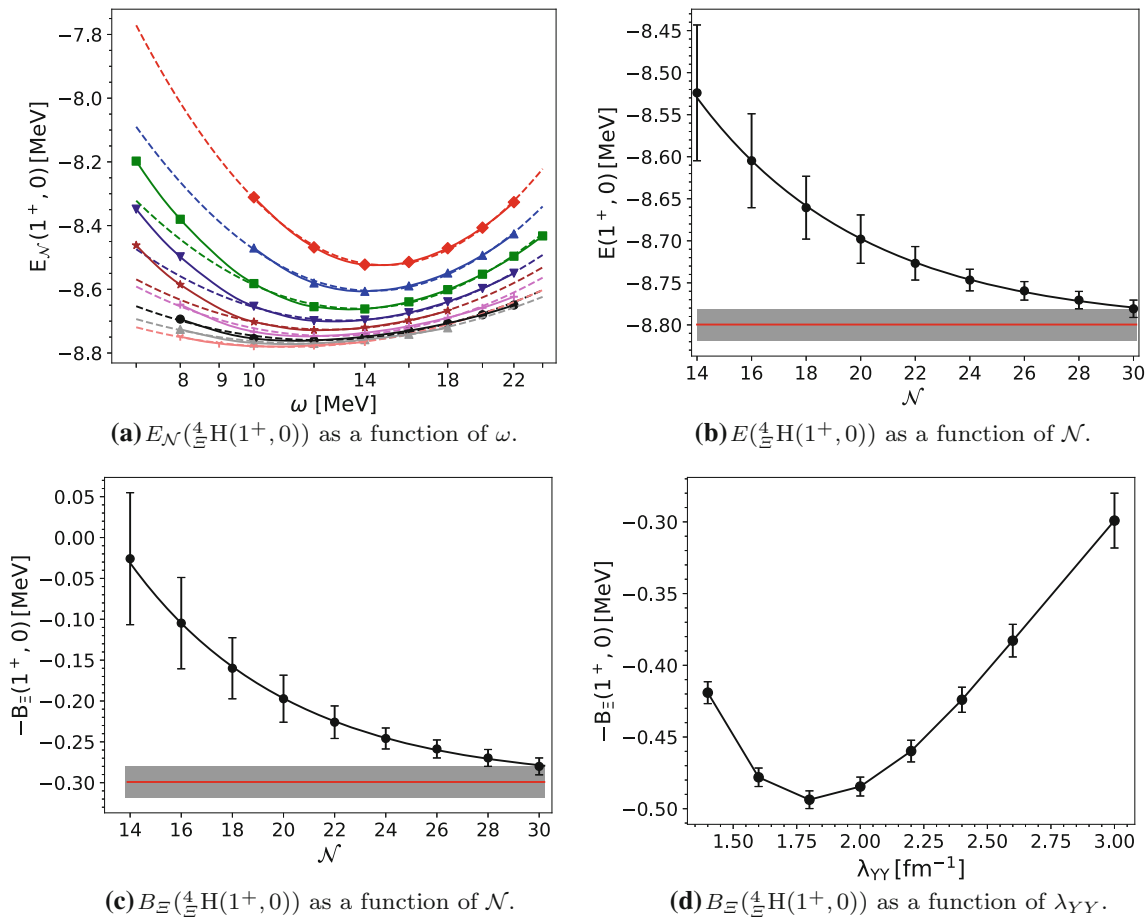
(a) $E_{\mathcal{N}}(^4_\Xi\mathrm{H}(1^+,0))$ as a function of ω.

(b) $E(^4_\Xi\mathrm{H}(1^+,0))$ as a function of $\mathcal{N}$.

(c) $B_\Xi(^4_\Xi\mathrm{H}(1^+,0))$ as a function of $\mathcal{N}$.

(d) $B_\Xi(^4_\Xi\mathrm{H}(1^+,0))$ as a function of λ_{YY}.

Fig. 2 a–c Binding energy E and Ξ separation energy B_Ξ for $^4_\Xi\mathrm{H}(1^+,0)$ computed with the YY-ΞN interaction NLO(500), SRG-evolved to a flow parameter of $\lambda_{YY} = 3.0$ fm^{-1}. For the NN interaction the SMS N^{4}LO+(450) potential [27] with $\lambda_{NN} = 1.6$ fm^{-1} is employed. B_Ξ is measured with respect to the triton binding energy (which is $E(^3\mathrm{H}) = -8.5$ MeV for the used NN interaction). **a** Solid lines and

symbols (with different colors) represent numerical results for different model spaces $\mathcal{N} = 14 - 30$, from top to bottom. The dashed lines are obtained by using the ansatz Eq. (22) in [36]. **b, c** Horizontal (red) lines with shaded areas indicate the converged results and the corresponding uncertainties. **d** Dependence of $B_\Xi(^4_\Xi\mathrm{H}(1^+,0))$ on the flow parameter λ_{YY}

Table 1 Ξ separation energies B_Ξ and estimated decay widths Γ for $A = 4 - 7$ Ξ hypernuclei. All calculations are based on the YY-ΞN interaction NLO(500) and the NN interaction SMS N^{4}LO+(450). Both potentials are SRG-evolved to a flow parameter of $\lambda_{NN} = \lambda_{YY} = 1.6$ fm^{-1}. The values of B_Ξ in NNNΞ, $^5_\Xi\mathrm{H}$ and $^7_\Xi\mathrm{H}$ are measured with respect to the binding energies of the core nuclei $^3\mathrm{H}$, $^4\mathrm{He}$ and $^6\mathrm{He}$, respectively

	B_Ξ [MeV]	Γ [MeV]
$^4_\Xi\mathrm{H}(1^+,0)$	0.48 ± 0.01	0.74
$^4_\Xi\mathrm{n}(0^+,1)$	0.71 ± 0.08	0.2
$^4_\Xi\mathrm{n}(1^+,1)$	0.64 ± 0.11	0.01
$^4_\Xi\mathrm{H}(0^+,0)$	–	–
$^5_\Xi\mathrm{H}(\frac{1}{2}^+,\frac{1}{2})$	2.16 ± 0.10	0.19
$^7_\Xi\mathrm{H}(\frac{1}{2}^+,\frac{3}{2})$	3.50 ± 0.39	0.2

to the strong ΞN interaction. The $\Xi^- p$ Coulomb interaction contributes roughly 200, 600, and 400 keV to the binding energies of NNNΞ, $^5_\Xi\mathrm{H}$ and $^7_\Xi\mathrm{H}$, respectively. Table 1 provides also an estimate of the corresponding decay width Γ. These widths have been evaluated perturbatively by adapting the procedure followed by Hiyama et al. [18,25]. Hiyama et al. have used the imaginary part of the G matrix. Here, we employ the ΞN T-matrix in the $^{11}S_0$ state from the original potential that includes the ΞN-$\Lambda\Lambda$ coupling [21] instead. Schematically the width amounts to $\Gamma \simeq -2\,\mathrm{Im}\,\langle \Psi_{B_\Xi} | T_{\Xi N - \Xi N} | \Psi_{B_\Xi} \rangle$ and involves the pertinent hypernuclear wave function Ψ_{B_Ξ} and the (off-shell) ΞN T-matrix at the sub-threshold energy corresponding to the bound state. One can clearly see that the three states $(1^+, 0)$, $(0^+, 1)$ and $(1^+, 1)$ in NNNΞ are only weakly bound, possessing quite similar B_Ξ's but substantially different decay widths. Interestingly, our result for $B_\Xi(\mathrm{NNN}\Xi(1^+, 0))$ is

close to that for the HAL QCD potential, reported in [18], although the $(0^+, 1)$ and $(1^+, 1)$ states are unbound for the HAL QCD interaction. There are substantial (but not surprising) differences between our separation energies $B_\Xi(\mathrm{NNN}\Xi)$ and the predictions [18] for the ESC08c potential [20]. According to the discussion in Ref. [18], it is the strong attraction in the $^{33}S_1$ and $^{13}S_1$ channels that is responsible for the rather large binding energies predicted for that ESC08c model in the $(1^+, 0)$ and $(1^+, 1)$ states.

Our results for the $^5_\Xi\mathrm{H}$ separation energy and decay width are $B_\Xi(^5_\Xi\mathrm{H}) = 2.16 \pm 0.1$ MeV and $\Gamma(^5_\Xi\mathrm{H}) = 0.19$ MeV, respectively. Oddly enough, these values agree roughly with the estimations by Myint and Akaishi [46] of 1.7 MeV and 0.2 MeV, respectively. However, given the differences in the underlying interactions and specifically in the employed approaches, this is certainly accidental. We further note that in contrast to our finding where $^5_\Xi\mathrm{H}$ is bound primarily due to the strong ΞN interaction, the authors in [46] state that the binding energy of 1.7 MeV in $^5_\Xi\mathrm{H}$ largely comes from the $^4\mathrm{He}\text{-}\Xi^-$ Coulomb interaction. The mechanism for the narrow width of $^5_\Xi\mathrm{H}$ has been investigated in [48,49]. Recently, Friedman and Gal, employing an optical potential, also reported a quite similar result for $^5_\Xi\mathrm{H}$ ($B_\Xi(^5_\Xi\mathrm{H}) = 2.0$ MeV) [11]. But also here the agreement could be more or less accidental given that the Ξ-nuclear interaction used as starting point in that work is with $U_\Xi \lesssim -20$ MeV significantly more attractive than the one predicted by the chiral ΞN potential employed in the present study which is only around $U_\Xi \approx -9$ MeV [38] as mentioned above.

The prediction of the chiral ΞN interaction for $^7_\Xi\mathrm{H}$ $(\frac{1}{2}^+, \frac{3}{2})$, $B_\Xi(^7_\Xi\mathrm{H}) = 3.50 \pm 0.39$ MeV, is only slightly larger than the binding energy of 3.15 MeV reported by Fujioka et al. [47,50] for the HAL QCD interaction, based on a calculation within a four-body $(\alpha nn\Xi)$ cluster model [25,51]. An earlier study utilizing older $S = -2$ potentials from the Nijmegen group indicated somewhat smaller binding energies [25,52]. Finally, as one can see from Table 1, the $^7_\Xi\mathrm{H}$ $(\frac{1}{2}^+, \frac{3}{2})$ state is also very narrow, with a width of $\Gamma = 0.2$ MeV.

To shed light on the relation between the properties of the chiral ΞN potential and the binding of the $A = 4 - 7$ Ξ systems, we provide in Table 2 the contributions of different ΞN partial waves to the expectation value of the $S = -2$ potential $\langle V^{S=-2} \rangle$. These results are computed at $\mathcal{N} = 28$, $\omega = 10$ MeV for NNNΞ, at $\mathcal{N} = 14$, $\omega = 16$ MeV for $^5_\Xi\mathrm{H}$ and at $\mathcal{N} = 10$, $\omega = 16$ MeV for $^7_\Xi\mathrm{H}$. Here the second largest model space is chosen for each system in order to save computational resources. And, ω is the corresponding optimal HO frequency for the chosen model space. For completeness, the energy expectation values are also shown in the last column of Table 2. Clearly, in all the considered states except NNN$\Xi(0^+, 0)$ the attractive ΞN interaction in the

$^{33}S_1$ channel plays the most important role in binding the systems. It accounts for more than 50% of the expectation value $\langle V^{s=-2} \rangle$. While the attraction in the $^{11}S_0$ channel is essential as well for NNN$\Xi(1^+, 0)$ and $(0^+, 1)$ (amounting to more than 30% of $\langle V^{S=-2} \rangle$), its contribution becomes less significant in other states. Furthermore, the ΞN repulsion in $^{31}S_0$ contributes predominantly to the expectation value $\langle V^{S=-2} \rangle$ of NNN$\Xi(0^+, 0)$ (naturally with opposite sign), which causes the system to be unbound. The expectation value $\langle V^{S=-2}(^{31}S_0) \rangle$ is also sizable for $^5_\Xi\mathrm{H}$ and $^7_\Xi\mathrm{H}$, however, its effect is largely canceled by the attraction in the $^{11}S_0$ channel.

Complementary to Table 2, the binding of the $A = 4 - 7$ hypernuclei can also be understood from Table 3, where probabilities of finding a ΞN pair, $P_{\Xi N}$, in different partial-wave states are listed. One clearly notices that, in most of the systems, a ΞN pair is predominantly found in those channels with $J \leq 1$ and in particular in the $^{33}S_1$, except for the unbound $^4_\Xi\mathrm{H}(0^+, 0)$ state. In addition, the two extremely small probabilities $P_{\Xi N}(^{11}S_0) = 0.02\%$ and $P_{\Xi N}(^{33}S_1) = 0.11\%$ in $^4_\Xi\mathrm{H}(0^+, 0)$ are obvious manifestations of the small expectation values $V^{S=-2}(^{11}S_0) = -0.002$ MeV and $V^{S=-2}(^{33}S_1) = -0.006$ MeV listed in Table 2. Furthermore, the strong variation of $P_{\Xi N}(^{11}S_0)$ in different states of the $A = 4 - 7$ hypernuclei clearly explains the large difference in the decay widths estimated for these systems, see Table 1.

As discussed in Sect. 2, we had to omit the $\Lambda\Lambda - \Xi N$ coupling in the J-NCSM application and we compensated that by a small modification of the ΞN potential strength in the $^{11}S_0$ state. It is reassuring to see that the overall effect of this partial wave on the binding energies is not too large. Specifically, the existence of the predicted bound states does not depend on its precise contribution, as can be read off from Tables 2 and 3. In fact, the slightly more attractive $^{11}S_0$ interaction predicted by the original ΞN potential, see Fig. 1, implies that all found Ξ hypernuclei could be simply minimally more bound.

Yet another view on the relation between the ΞN interaction and the binding of s-shell Ξ hypernuclei is given in Appendix A, in terms of appropriately averaged effective ΞN interactions, analogous to what has been done for the ΛN interaction and s-shell Λ hypernuclei in the past [53]. Although those simple relations are only approximately valid, they nevertheless help to understand the results presented in Tables 2 and 3.

5 Conclusions

In this work, we employed the Jacobi NCSM in combination with the chiral NLO(500) ΞN potential to explore $A = 4 - 7$ Ξ hypernuclei. Particle conversions like $\Lambda\Sigma - \Xi N - \Sigma\Sigma$

Table 2 Contributions of different partial waves to $\langle V^{S=-2} \rangle$ (first five columns), and the total binding energy (last column) for the $A = 4 - 7$ Ξ hypernuclei. The results are extracted at $\mathcal{N} = 28$, $\omega = 10$ MeV for NNNΞ, at $\mathcal{N} = 14$, $\omega = 16$ MeV for $^5_\Xi$H and at $\mathcal{N} = 10$, $\omega = 16$ MeV for $^7_\Xi$H. All energies are given in MeV. Same interactions as in Table 1. Note that the calculated binding energy of ^{3}He(^{3}H) is $-7.79\,(-8.50)$ MeV

	$V^{S=-2}$					E
	$^{11}S_0$	$^{31}S_0$	$^{13}S_1$	$^{33}S_1$	Total	
$^4_\Xi$H$(1^+, 0)$	-1.95	0.02	-0.7	-2.31	-5.21	-8.97
$^4_\Xi$n$(0^+, 1)$	-0.6	0.25	-0.004	-0.74	-1.37	-9.07
$^4_\Xi$n$(1^+, 1)$	-0.02	0.16	-0.13	-1.14	-1.30	-9.0
$^4_\Xi$H$(0^+, 0)$	-0.002	0.08	-0.01	-0.006	-0.11	-6.94
$^5_\Xi$H$(1/2^+, 1/2)$	-0.96	0.94	-0.58	-3.63	-4.88	-31.43
$^7_\Xi$H$(1/2^+, 3/2)$	-1.23	1.79	-0.79	-6.74	-8.04	-33.22

Table 3 Probabilities (in %) of finding a ΞN pair in different partial-wave states in the wave functions of $A = 4 - 7$ Ξ hypernuclei. Same interactions and model spaces as in Table 1. Note that for each system all probabilities sum up to the probability of finding a Ξ hyperon in that system

	$|\Xi N\rangle$				
	$|^{11}S_0\rangle$	$|^{31}S_0\rangle$	$|^{13}S_1\rangle$	$|^{33}S_1\rangle$	$J \geq 2$
$^4_\Xi$H$(1^+, 0)$	12.88	0.18	25.91	35.72	24.80
$^4_\Xi$n$(0^+, 1)$	8.24	13.32	0.23	23.29	54.73
$^4_\Xi$n$(1^+, 1)$	0.14	9.22	9.83	33.08	47.56
$^4_\Xi$H$(0^+, 0)$	0.02	11.87	14.65	0.11	73.33
$^5_\Xi$H$(1/2^+, 1/2)$	4.82	12.18	14.37	35.53	32.59
$^7_\Xi$H$(1/2^+, 3/2)$	3.71	12.92	11.11	38.36	32.94

are fully taken into account, while the transition $\Lambda\Lambda - \Xi$N is omitted and its contribution is incorporated effectively by re-adjusting the strength of the $V_{\Xi N}$ potential appropriately. The latter approach facilitates a proper convergence of the energy calculations to the lowest lying Ξ states. Furthermore, to speed up the convergence, the ΞN potential is SRG-evolved to a wide range of flow parameters. The effect of SRG evolution on the Ξ separation energies is in general small, but, it is slightly larger than that observed for $\Lambda\Lambda$ hypernuclei. We found three loosely bound states $(1^+, 0)$, $(0^+, 1)$ and $(1^+, 1)$ for the NNNΞ system and more tightly bound $^5_\Xi$H, $^7_\Xi$H hypernuclei. These Ξ systems are bound predominantly due to the attraction of the chiral ΞN potential in the $^{33}S_1$ channel. On the other hand, the repulsive nature in $^{31}S_0$ prevents the binding of the NNN$\Xi\,(0^+, 0)$ state. All the investigated Ξ bound states are predicted to have very small decay widths.

In view of these results, which are based on an interaction that is fully consistent with presently available experimental constraints, and well in line with current lattice QCD results [22], it seems likely that light Ξ hypernuclei exist. Experimental confirmation is certainly challenging. However, the-oretical estimates for yields of $A = 4$ hypernuclei [54] as well as actual measurements of $^4_\Lambda$H, $^4_\Lambda$He by the STAR Collaboration [55] raise hopes that NNNΞ bound states can be detected in heavy ion collisions in the not too far future. Also a bound $^7_\Xi$H system could be produced and studied in the ^{7}Li(K^-, K^+) reaction [25], cf. the proposal P75 for J-PARC [52]. Once these new experimental results are available, they will provide new insights into the properties of $S = -2$ BB interactions. The current manuscript sets up a framework that allows one to exploit these insights to constrain BB interactions in the future.

Appendix A: Estimate of partial wave contributions

In this appendix, we present approximately valid expressions for the partial-wave contributions of the ΞN interaction to s-shell Ξ hypernuclei. The relations are derived in a similar way as the ones for the ΛN interaction and Λ hypernuclei [53]. For these estimates it is assumed that there is no particle conversion. Additionally, the Ξ hypernuclei should exhibit a clear core-Ξ structure. Both, the core nucleons and the Ξ are in s-wave states. Those assumptions are indeed justified, as one can see from Tables 4 and 5 where we provide probabilities of finding the nucleons in certain angular momentum and isospin states and together with Ξ^- or Ξ^0. For the isospin zero states of $A = 4$, the hypernucleus seems to be dominated by the $^3\mathrm{He}/^3\mathrm{H}$ component together with Ξ^- and Ξ^0, respectively. The choice of $T = 0$ enforces that both parts contribute equally. For the other isospin and $A = 5$ and 7, the total charge of the systems is chosen such that the Ξ^- contribution dominates in conjunction with the expected core nuclei. In the approximation that the hypernucleus only contains these dominant components, one obtains for the effective interactions

$$\begin{aligned}
&{}^3_\Xi\mathrm{H}(\tfrac{1^+}{2}, \tfrac{1}{2}) : \tilde{V}_{\Xi N} \\
&\approx \frac{3}{16} V_{\Xi N}^{11 S_0} + \frac{9}{16} V_{\Xi N}^{31 S_0} + \frac{1}{16} V_{\Xi N}^{13 S_1} + \frac{3}{16} V_{\Xi N}^{33 S_1} \quad (\mathrm{A.1})
\end{aligned}$$

$$
{}^3_\Xi\mathrm{H}(\tfrac{3^+}{2}, \tfrac{1}{2}) : \tilde{V}_{\Xi N} \approx \frac{1}{4} V_{\Xi N}^{13 S_1} + \frac{3}{4} V_{\Xi N}^{33 S_1} \quad (\mathrm{A.2})
$$

$$
{}^4_\Xi\mathrm{H}(1^+, 0) : \tilde{V}_{\Xi N} \approx \frac{1}{6} V_{\Xi N}^{11 S_0} + \frac{1}{3} V_{\Xi N}^{13 S_1} + \frac{1}{2} V_{\Xi N}^{33 S_1} \quad (\mathrm{A.3})
$$

$$
{}^4_\Xi\mathrm{H}(0^+, 1) : \tilde{V}_{\Xi N} \approx \frac{1}{6} V_{\Xi N}^{11 S_0} + \frac{1}{3} V_{\Xi N}^{31 S_0} + \frac{1}{2} V_{\Xi N}^{33 S_1} \quad (\mathrm{A.4})
$$

$$
{}^4_\Xi\mathrm{H}(1^+, 1) : \tilde{V}_{\Xi N} \approx \frac{1}{6} V_{\Xi N}^{31 S_0} + \frac{1}{6} V_{\Xi N}^{13 S_1} + \frac{2}{3} V_{\Xi N}^{33 S_1} \quad (\mathrm{A.5})
$$

$$
{}^4_\Xi\mathrm{H}(0^+, 0) : \tilde{V}_{\Xi N} \approx \frac{1}{2} V_{\Xi N}^{31 S_0} + \frac{1}{2} V_{\Xi N}^{13 S_1} \quad (\mathrm{A.6})
$$

$$\begin{aligned}
{}^5_\Xi\mathrm{H}(\tfrac{1^+}{2}, \tfrac{1}{2}) : \tilde{V}_{\Xi N} &\approx \frac{1}{16} V_{\Xi N}^{11 S_0} + \frac{3}{16} V_{\Xi N}^{31 S_0} \\
&+ \frac{3}{16} V_{\Xi N}^{13 S_1} + \frac{9}{16} V_{\Xi N}^{33 S_1}. \quad (\mathrm{A.7})
\end{aligned}$$

It clearly follows from Eqs. (A.1–A.7) that the $^{33}S_1$ ΞN interaction dominates the $(\tfrac{3^+}{2}, \tfrac{1}{2})$ state in $^3_\Xi\mathrm{H}$, the $(1^+, 0)$, $(0^+, 1)$ and $(1^+, 1)$ states in NNNΞ and the $^5_\Xi\mathrm{H}$ hypernucleus. Since it is attractive, cf. Fig. 1, it is predominantly responsible for the binding of the latter four hypernuclei, see Tables 2 and 3. The $^{31}S_0$ partial wave is dominant in $^3_\Xi\mathrm{H}(\tfrac{1^+}{2}, \tfrac{1}{2})$, and since it is repulsive no bound state can be expected [18,19]. In the case of NNNΞ $(0^+, 0)$, which is likewise found unbound in our calculation and in [18], the (more strongly) repulsive $^{31}S_0$ and the weakly attractive $^{13}S_1$ potentials contribute practically with equal weights.

Table 4 Probabilities (in %) of finding the nucleons in a total J_{core} and T_{core} angular momentum and isospin state and with a Ξ hyperon with third component of isospin m_Ξ^t in the wave functions of $A = 4$ Ξ hypernuclei

$(J_{core}, T_{core}, m_\Xi^t)$	${}^4_\Xi H(1^+, 0)$	${}^4_\Xi n(0^+, 1)$	${}^4_\Xi n(1^+, 1)$	${}^4_\Xi H(0^+, 0)$
$(\tfrac{1}{2}, \tfrac{1}{2}, -\tfrac{1}{2})$	49.66	97.48	97.44	49.98
$(\tfrac{1}{2}, \tfrac{1}{2}, \tfrac{1}{2})$	49.66	–	–	49.98
$(\tfrac{1}{2}, \tfrac{3}{2}, \tfrac{1}{2})$	–	0.54	0.55	–
$(\tfrac{1}{2}, \tfrac{3}{2}, -\tfrac{1}{2})$	–	1.6	1.6	–
others	0.16	0.17	0.22	0.02

Table 5 Same as Table 4 for $A = 5$ and 7 Ξ hypernuclei

$(J_{core}, T_{core}, m_\Xi^t)$	${}^5_\Xi H(\tfrac{1^+}{2}, \tfrac{1}{2})$	$(J_{core}, T_{core}, m_\Xi^t)$	${}^7_\Xi H(\tfrac{1^+}{2}, \tfrac{3}{2})$
$(0, 0, -\tfrac{1}{2})$	96.03	$(0, 1, -\tfrac{1}{2})$	94.44
$(0, 0, \tfrac{1}{2})$	1.1	$(0, 2, -\tfrac{1}{2})$	0.7
$(0, 1, \tfrac{1}{2})$	2.1	$(0, 2, \tfrac{1}{2})$	2.8
others	0.3	others	1.13

References

1. E. Hiyama, K. Nakazawa, Structure of $S = -2$ hypernuclei and hyperon–hyperon interactions. Ann. Rev. Nucl. Part. Sci. **68**, 131–159 (2018). https://doi.org/10.1146/annurev-nucl-101917-021108

2. K. Nakazawa et al., The first evidence of a deeply bound state of $\Xi^- - {}^{14}$N system. PTEP **2015**(3), 033D02 (2015). https://doi.org/10.1093/ptep/ptv008

3. S.H. Hayakawa et al., Observation of coulomb-assisted nuclear bound state of $\Xi^- - {}^{14}$N system. Phys. Rev. Lett. **126**, 062501 (2021). https://doi.org/10.1103/PhysRevLett.126.062501

4. M. Yoshimoto et al., First observation of a nuclear s-state of a Ξ hypernucleus, ${}^{15}_{\Xi}$C. PTEP **2021**(7), 073D02 (2021). https://doi.org/10.1093/ptep/ptab073

5. T. Nagae et al., Observation of a Xi bound state in the ${}^{12}C(K^-, K^+)$ reaction at 1.8 GeV/c. AIP Conf. Proc. **2130**(1), 020015 (2019). https://doi.org/10.1063/1.5118383

6. S. Acharya et al., First observation of an attractive interaction between a proton and a cascade baryon. Phys. Rev. Lett. **123**(11), 112002 (2019). https://doi.org/10.1103/PhysRevLett.123.112002 arXiv:1904.12198

7. S. Acharya et al., Unveiling the strong interaction among hadrons at the LHC. Nature **588**, 232–238 (2020). https://doi.org/10.1038/s41586-020-3001-6 arXiv:2005.11495

8. T.T. Sun, E. Hiyama, H. Sagawa, H.J. Schulze, J. Meng, Mean field approaches for Ξ^- hypernuclei and current experimental data. Phys. Rev. C **94**(6), 064319 (2016). https://doi.org/10.1103/PhysRevC.94.064319 arXiv:1611.03661

9. Y. Jin, X.-R. Zhou, Y.-Y. Cheng, H.J. Schulze, Study of Ξ^- hypernuclei in the Skyrme–Hartree–Fock approach. Eur. Phys. J. A **56**(5), 135 (2020). https://doi.org/10.1140/epja/s10050-020-00143-7 arXiv:1910.05884

10. R. Shyam, K. Tsushima, Description of the recently observed hypernucleus ${}^{15}_{\Xi^-}$C within a quark-meson coupling model. **1** (2019). arXiv:1901.06090

11. E. Friedman, A. Gal, Constraints on Ξ^- nuclear interactions from capture events in emulsion. Phys. Lett. B **820**, 136555 (2021). https://doi.org/10.1016/j.physletb.2021.136555 arXiv:2104.00421

12. M. Kohno, K. Miyagawa, Ξ hyper-nuclear states predicted by NLO chiral baryon–baryon interactions. **7** (2021). arxiv: 2107.03784

13. J. Hu, H. Shen, Y. Zhang, The ΞN interaction constrained by recent Ξ^- hypernuclei experiments. **4** (2021.) arXiv:2104.13567

14. H. Takahashi et al., Observation of a ${}^6_{\Lambda\Lambda}$He double hypernucleus. Phys. Rev. Lett. **87**, 212502 (2001). https://doi.org/10.1103/PhysRevLett.87.212502

15. K. Nakazawa, Double-lambda hypernuclei via the Xi-hyperon capture at rest reaction in a hybrid emulsion. Nucl. Phys. A **835**, 207–214 (2010). https://doi.org/10.1016/j.nuclphysa.2010.01.195

16. H. Garcilazo, A. Valcarce, Deeply bound Ξ tribaryon. Phys. Rev. C **93**(3), 034001 (2016). https://doi.org/10.1103/PhysRevC.93.034001 arXiv:1605.04108

17. I. Filikhin, V.M. Suslov, B. Vlahovic, Faddeev calculations for light Ξ-hypernuclei. Math. Model. Geom. **5**(2), 1–11 (2017). arXiv:1705.03446

18. E. Hiyama, K. Sasaki, T. Miyamoto, T. Doi, T. Hatsuda, Y. Yamamoto, Th.A. Rijken, Possible lightest Ξ hypernucleus with modern ΞN interactions. Phys. Rev. Lett. **124**(9), 092501 (2020). https://doi.org/10.1103/PhysRevLett.124.092501 arXiv:1910.02864

19. K. Miyagawa, M. Kohno, A realistic approach to the ΞNN bound-state problem based on Faddeev equation. Few Body Syst. **62**, 65 (2021). https://doi.org/10.1007/s00601-021-01650-z arXiv:2105.11258

20. M. M. Nagels, Th. A. Rijken, Y. Yamamoto, Extended-soft-core baryon–baryon ESC08 model III. S = - 2 hyperon–hyperon/nucleon interaction. 2015. arXiv:1504.02634

21. J. Haidenbauer, U.-G. Meißner, In-medium properties of a ΞN interaction derived from chiral effective field theory. Eur. Phys. J. A **55**(2), 23 (2019). arXiv:1810.04883

22. K. Sasaki et al., $\Lambda\Lambda$ and $N\Xi$ interactions from lattice QCD near the physical point. Nucl. Phys. A **998**, 121737 (2020). https://doi.org/10.1016/j.nuclphysa.2020.121737 arXiv:1912.08630

23. J. Haidenbauer, U.-G. Meißner, S. Petschauer, Strangeness $S = -2$ baryon–baryon interaction at next-to-leading order in chiral effective field theory. Nucl. Phys. A **954**, 273–293 (2016). https://doi.org/10.1016/j.nuclphysa.2016.01.006 arXiv:1511.05859

24. Emiko Hiyama, Gaussian expansion method for few-body systems and its applications to atomic and nuclear physics. PTEP **2012**, 01A204 (2012). https://doi.org/10.1093/ptep/pts015

25. E. Hiyama, Y. Yamamoto, T. Motoba, Th.A. Rijken, M. Kamimura, Light Xi hypernuclei in four-body cluster models. Phys. Rev. C **78**, 054316 (2008). https://doi.org/10.1103/PhysRevC.78.054316 arXiv:0811.3156

26. E. Epelbaum, H. Hammer, U.-G. Meißner, Modern theory of nuclear forces. Rev. Mod. Phys. **81**, 1773–1825 (2009). https://doi.org/10.1103/RevModPhys.81.1773 arXiv:0811.1338

27. P. Reinert, H. Krebs, E. Epelbaum, Semilocal momentum-space regularized chiral two-nucleon potentials up to fifth order. Eur. Phys. J. A **54**(5), 86 (2018). https://doi.org/10.1140/epja/i2018-12516-4 arXiv:1711.08821

28. E. Epelbaum et al., Few- and many-nucleon systems with semilocal coordinate-space regularized chiral two- and three-body forces. Phys. Rev. C **99**(2), 024313 (2019). arXiv:1807.02848

29. M. Piarulli et al., Light-nuclei spectra from chiral dynamics. Phys. Rev. Lett. **120**(5), 052503 (2018). arXiv:1707.02883

30. E. Epelbaum et al., Towards high-order calculations of three-nucleon scattering in chiral effective field theory. Eur. Phys. J. A **56**(3), 92 (2020). https://doi.org/10.1140/epja/s10050-020-00102-2 arXiv:1907.03608

31. P. Maris et al., Light nuclei with semilocal momentum-space regularized chiral interactions up to third order. Phys. Rev. C **103**, 054001 (2021). https://doi.org/10.1103/PhysRevC.103.054001 arXiv:2012.12396

32. Henk Polinder, Johann Haidenbauer, Ulf-G. Meißner, Hyperon nucleon interactions: a chiral effective field theory approach. Nucl. Phys. A **779**, 244–266 (2006). https://doi.org/10.1016/j.nuclphysa.2006.09.006

33. J. Haidenbauer, S. Petschauer, N. Kaiser, U.-G. Meißner, A. Nogga, W. Weise, Hyperon–nucleon interaction at next-to-leading order in chiral effective field theory. Nucl. Phys. A **915**, 24–58 (2013). https://doi.org/10.1016/j.nuclphysa.2013.06.008 arXiv:1304.5339

34. J. Haidenbauer, U.-G. Meißner, A. Nogga, Hyperon–nucleon interaction within chiral effective field theory revisited. Eur. Phys. J. A **56**(3), 91 (2020). https://doi.org/10.1140/epja/s10050-020-00100-4 arXiv:1906.11681

35. H. Le, J. Haidenbauer, U.-G. Meißner, A. Nogga, Implications of an increased Λ-separation energy of the hypertriton. Phys. Lett. B **801**, 135189 (2020). https://doi.org/10.1016/j.physletb.2019.135189 arXiv:1909.02882

36. H. Le, J. Haidenbauer, U.-G. Meißner, A. Nogga, Jacobi no-core shell model for p-shell hypernuclei. Eur. Phys. J. A **8** (2020.) arXiv:2008.11565 https://doi.org/10.1140/epja/s10050-020-00314-6

37. H. Le, J. Haidenbauer, U.-G. Meißner, A. Nogga, S-shell $\Lambda\Lambda$ hypernuclei based on chiral interactions. Eur. Phys. J. A **57**, 217 (2021). https://doi.org/10.1140/epja/s10050-021-00522-8

38. M. Kohno, Ξ hyperons in the nuclear medium described by chiral NLO interactions. Phys. Rev. C **100**(2), 024313 (2019). https://doi.org/10.1103/PhysRevC.100.024313 arXiv:1908.01934

39. P. Khaustov et al., Evidence of Xi hypernuclear production in the C-12(K-, K+)(Xi)Be-12 reaction. Phys. Rev. C **61**, 054603 (2000). https://doi.org/10.1103/PhysRevC.61.054603 arXiv:nucl-ex/9912007

40. A. Gal, E.V. Hungerford, D.J. Millener, Strangeness in nuclear physics. Rev. Mod. Phys. **88**(3), 035004 (2016). https://doi.org/10.1103/RevModPhys.88.035004 arXiv:1605.00557

41. H. Polinder, J. Haidenbauer, U.-G. Meißner, Strangeness $S = -2$ baryon–baryon interactions using chiral effective field theory. Phys. Lett. B **653**, 29–37 (2007). arXiv:0705.3753

42. J. Haidenbauer, U.-G. Meißner, To bind or not to bind: the H-dibaryon in light of chiral effective field theory. Phys. Lett. B **706**, 100–105 (2011). https://doi.org/10.1016/j.physletb.2011.10.070 arXiv:1109.3590

43. S. K. Bogner, Richard J. Furnstahl, R. J. Perry, Similarity renormalization group for nucleon–nucleon interactions. Phys. Rev. **C 75**(6), 061001 (2007). https://doi.org/10.1103/PhysRevC.75.061001

44. B. Wiringa, V.G.J. Stoks, R. Schiavilla, An accurate nucleon–nucleon potential with charge independence breaking. Phys. Rev. C **51**, 38 (1995). https://doi.org/10.1103/PhysRevC.51.38 arXiv:nucl-th/9408016

45. S. Liebig, U.-G. Meißner, A. Nogga, Jacobi no-core shell model for p-shell nuclei. Eur. Phys. J. A **52**(4), 103 (2016). https://doi.org/10.1140/epja/i2016-16103-5 arXiv:1510.06070

46. K.S. Myint, Y. Akaishi, Double strangeness five-body system. Prog. Theor. Phys. Suppl. **117**, 251–264 (1994). https://doi.org/10.1143/PTP.117.251

47. H. Fujioka et al., Search for the lightest double-Λ Hypernucleus, $^{5}_{\Lambda\Lambda}$H, at J-PARC. Few Body Syst. **62**, 47 (2021). [Erratum: Few Body Syst. 62, 69 (2021)]. https://doi.org/10.1007/s00601-021-01654-9

48. C.B. Dover, D.J. Millener, A. Gal, On the production and decay of strangeness S = - 2 hypernuclei. Nucl. Phys. A **572**, 85–111 (1994). https://doi.org/10.1016/0375-9474(94)90423-5

49. I. Kumagai-Fuse, Y. Akaishi, Narrow width mechanism of A = 5 Ξ-state. Prog. Theor. Phys. **94**, 151–156 (1995). https://doi.org/10.1143/PTP.94.151

50. H. Fujioka, Contribution to the 8th Asia-Pacific conference on few-body problems in physics (APFB2021). https://indico.rcnp.osaka-u.ac.jp/event/1457/contributions/7863/attachments/6107/7399/fujioka_APFB2020_pub.pdf (2021)

51. E. Hiyama. Private communication

52. H. Fujioka, T. Fukuda, E. Hiyama, et al., Phase-1 of the P75 experiment: measurement of the formation cross section of $^{7}_{\Xi^-}$H in the ^{7}Li(K^-, K^+) reaction. (2019). http://j-parc.jp/researcher/Hadron/en/pac_1901/pdf/P75_2019-09.pdf and http://j-parc.jp/researcher/Hadron/en/pac_2001/pdf/P75_2020-02.pdf

53. B.F. Gibson, I.R. Afnan, J.A. Carlson, D.R. Lehman, Importance of baryon baryon coupling in hypernuclei. Prog. Theor. Phys. Suppl. **117**, 339–350 (1994). https://doi.org/10.1143/PTPS.117.339 arXiv:nucl-th/9411027

54. J. Steinheimer, K. Gudima, A. Botvina, I. Mishustin, M. Bleicher, H. Stocker, Hypernuclei, dibaryon and antinuclei production in high energy heavy ion collisions: thermal production versus coalescence. Phys. Lett. B **714**, 85–91 (2012). https://doi.org/10.1016/j.physletb.2012.06.069 arXiv:1203.2547

55. H. Leung. Contribution to the 19th Conference on Strangeness in Quark Matter (SQM2021). https://indico.cern.ch/event/985652/contributions/4296086/attachments/2248875/3814733/sqm2021hypernucleiv7.pdf (2021)